Indian Journal of Chemical Technology
Vol. 30, May 2023, pp. 308-319
DOI: 10.56042/ijct.v30i3.70100

Carboxymethylated gum tragacanth crosslinked poly(sodium acrylate)hydrogel: Fabrication, characterization, rheology and drug-delivery application

Meenakshi Tanwar, Rajinder K Gupta* & Archna Rani*
Department of Applied Chemistry, Delhi Technological University, Delhi 110 042, India
E-mail:rkg67ap@yahoo.com,

Received 5 January 2023; accepted 16 February 2023

This study aimed to synthesize Carboxymethylated Gum Tragacanth (CMGT) from the Gum Tragacanth (GT). Modified gum's potential as a drug delivery carrier has been explored by synthesizing CMGT based hydrogels. The viscoelastic characteristics of the fabricated hydrogel have been examined by Rheological analysis. SEM studies have been conducted to examine the surface morphology and TGA is used to perform the thermal analysis. XRD, FTIR, and solid state ^{13}C NMR have been used to examine the structural features of the GT, CMGT, sodium acrylate based hydrogel (SAH) and carboxymethylated gum tragacanth co-polymerized with sodium acrylate based hydrogel (CMGT-co-SAH). The anti-inflammatory drug, Aceclofenac Sodium(AFS) loaded onto the hydrogel has been used as a model drug. The AFS follows the Fickian mechanism of diffusion and the results are best fitted in Higuchi and Korsmeyer–Peppas models.

Keywords: *Astragalus gummifer*, Carboxymethylation, Drug-delivery, Hydrogel, Polysaccharides

An excellent way to increase the drug's effectiveness is to deliver it using any reliable carrier in medical science. In this modern period, natural gum polysaccharides are explored as the main component in pharmaceutical formulations[1–3]. Recently, the potential of Gum Tragacanth has been explored in cosmetics, pharmaceuticals, bio and food industries[4,5]. The GT obtained from *Astragalus gummifer* is considered GRAS (Generally Recognized As Safe)[6]. GT is a heterogeneous, anionic and naturally available polysaccharide. The presence of arabinogalactan in GT was confirmed by acid hydrolysis[7]. In traditional local medications, GT act as a demulcent for gastrointestinal problems and sore throats. It may additionally have analgesic properties[8]. The property of the GT can be enhanced through chemical modifications, as previously reported in the literature. The reported modification methods of GT are graft-copolymerization[9] and carboxymethylation[10]. However, carboxy-methylation is most widely favoured as it is cheap, quickly processed and produces versatile products with better water retention properties and strength[11] compared to natural ones[12]. In the current study, GT was carboxymethylated to synthesize CMGTand the potential of CMGT in drug delivery was further investigated by synthesizing CMGT based hydrogel.

The three-dimensional network structure of a hydrogel has been created by the chemical cross-linking of polysaccharides with suitable monomer by using a suitable initiator and multifunctional cross-linker. In the past few years, the hydrogel has increasingly been utilized as a carrier in drug delivery application to produce sustained and controlled drug release because of its 3Dweb structure and excellent swelling property[13,14].

The swell ability of the hydrogel can be enhanced by using sodium acrylate (SA) content in the graft polymerization[15]. Ganguly *et al*. also observed the same swellability of the hydrogel based on psyllium gum copolymerized with acrylic acid and sodium acrylate[16]. The application of CMGT in the preparation of superabsorbent hydrogel has been reported by Mohammad B *et al.*[17]. Previous literature reveals that CMGT based hydrogel and their application in drug delivery is still to be explored. In this study, we have synthesized and characterized the novel AFS loaded hydrogel based on graft co-polymerization of SA onto the CMGT backbone. The various formulations of CMGT-co-SAH were synthesized by varying the amount of KPS as initiator and MBA as cross-linker, and their swelling Index (SI) was assessed. Also, by changing the temperature, i.e., 27, 37 and 47°C, SI and network parameters of the hydrogel were determined. Modification of the GT to CMGT and their graft copolymerization with SA was confirmed by XRD, FTIR, TGA, SEM and C^{13}-NMR. Rheological analysis

of the SAH, which is considered as control hydrogel and CMGT-co-SAH were done to determine the gel characteristics. Further, the drug release behaviour of the CMGT-co-SAH was evaluated by using a model drug, AFS by applying different kinetic models such as Hixon-Crowell, Higuchi, Korsmeyer-Peppas, Zero-order and First-order kinetic model to analyse the drug release profile.

Experimental Section

Materials

GT(purchased from local market, New Delhi), Sodium monochloroacetate (SMCA, CDH, New Delhi), N,N′-methylenebis-acrylamide (MBA, CDH, New Delhi),Sodium hydroxide (NaOH, Fischer Scientific, Mumbai), Acrylic acid (AA, CDH, New Delhi), Potassium per sulphate (KPS, Fischer Scientific, Mumbai), Iso propyl alcohol(Fischer Scientific, Mumbai), methanol (Fischer Scientific, Mumbai), AFS was gifted from Unicure India Pvt. Ltd. and all the solutions were prepared in milli-Q grade distilled water.

Synthesis of Carboxymethylated Gum Tragacanth (CMGT)

The CMGT was synthesized using a previously described method[12] with slight modifications in the procedure. Derivatization of the polysaccharides chain follows Williamson's synthesis reaction. For 0.2 degrees of substitution (0.2 DOS chosen for good swelling properties), the required amount of GT was weighed and mixed continuously for 15 min in distilled water. Then (0.00775 moles) of NaOH was added to the homogeneous solution of GT. After 30 min of stirring, SMCA (0.00123 moles) was gradually added. The solution was stirred at magnetic stirrer for 3 h at 70°C to make it homogeneous. Once the CMGT solution was cooled, the precipitates of CMGT were filtered, washed at least three times with isopropyl alcohol (80%), and oven dried at 45 °C.

Estimation of Degree of Substitution (DOS) on GT

DOS of CMGT was determined by back titration[18]. CMGT (1 g) was dispersed in the required volume of HCl and Isopropyl alcohol was added as a solvent. The stirring of the solution with a glass rod was carried out for 15 min to avoid the formation of lumps. The solution was left undisturbed for 20 min. Afterwards, distilled water was added and subjected to magnetic stirring for a few minutes. Post sedimentation, water was decanted. The sediment was filtered. Multiple washing was done with distilled water to free it from excess acid. A silver nitrate test was performed to check the presence of acid in the filtrate. Finally, the residue was divided into two accurately weighed parts. One part of the residue was dispersed in 0.1 N NaOH and subjected to magnetic stirring for 30 min before back titrating with 0.1 N HCl. The dried content was calculated after drying the other part of the residue.

Equations (1 and 2) were used to calculate DOS[19].

$$\mathrm{DOS} = \frac{0.162\mathrm{A}}{1-0.058\mathrm{A}} \quad \ldots (1)$$

Where

$$\mathrm{A} = \frac{(mL\ of\ NaOH \times N1) - (mL\ of\ HCl \times N2)}{g\ of\ the\ dried\ sample} \quad \ldots (2)$$

N1 and N2 represent the normalities of NaOH and HCl, and A represents (milliequivalents of NaOH /g of sample).

Synthesis of CMGT-co-SAH

CMGT-co-SAH was synthesized by taking required amount of CMGT with DOS (0.2) (0.33% w/v) in distilled water. 7.2 mL of acrylic acid (AA) was neutralized using 13 mL of 8.07 mol/L NaOH solution and added to CMGT solution. At room temperature, KPS (0.0061 mol/L) and MBA (0.017 mol/L) were added to the aqueous reaction with continuous stirring for 2 h on a magnetic stirrer. The polymerization procedure was carried out in a water bath at 60°C for 2 h. The synthesized hydrogel was washed with an organic/aqueous solvent to remove the soluble components. It was then dried in the hot air oven at 45°C, till constant weight. Reaction contents were optimized by varying the amount of reactants; KPS0.0061 mol/L to 0.01223 mol/L and MBA0.010 mol/L to 0.021 mol/L (Table 1). Optimal formulation of hydrogel (i.e., CMGT-co-SAH-4) was selected for further characterization based on the highest swelling Index among various compositions(CMGT-co-SAH-1 to 11).

Characterization and analysis

Swelling studies

Effect of cross-linker, initiator and the temperature on hydrogel's network was analyzed by the swelling equilibrium method in buffer solution of *p*H 7.4. The oven dried and weighed discs of hydrogel were dipped in the solvent. After a fixed interval, the hydrogel discs were removed from the swelling medium, extra fluid was tapped with tissue paper, and weighed again until the constant weight was obtained.

Table 1 — Different formulation of CMGT-co-SAH and their swelling Index.

Formulation	Polymer(CMGT)(g)	Monomer(AAc)(g)	NaOH (mol/l)	Initiator(KPS) (mol/L)	Cross-linker (MBA)(mol/L)	Swelling Index g/g of gel) (After 24 h)
CMGT-co-SAH-1	0.1	7.2	8.07	0.0061	0.01	22.28±0.27
CMGT-co-SAH-2	0.1	7.2	8.07	0.0061	0.012	23.29±0.17
CMGT-co-SAH-3	0.1	7.2	8.07	0.0061	0.015	28.95±0.02
CMGT-co-SAH-4	0.1	7.2	8.07	0.0061	0.017	33.13±0.04
CMGT-co-SAH-5	0.1	7.2	8.07	0.0061	0.019	27.13±0.08
CMGT-co-SAH-6	0.1	7.2	8.07	0.0061	0.021	25.74±0.25
CMGT-co-SAH-7	0.1	7.2	8.07	0.0074	0.01	26.92±0.56
CMGT-co-SAH-8	0.1	7.2	8.07	0.0074	0.012	30.45±0.04
CMGT-co-SAH-9	0.1	7.2	8.07	0.0086	0.01	30.25±0.19
CMGT-co-SAH-10	0.1	7.2	8.07	0.0086	0.015	27.67±0.02
CMGT-co-SAH-11	0.1	7.2	8.07	0.0098	0.01	26.26±0.50

These studies were done in triplicate. Equation 3 was used to calculate the swelling index (SI)[20].

$$SI\% = \frac{Ws-Wi}{Wi} \times 100 \quad \ldots (3)$$

Wi represents the dried hydrogel disc's weight, whereas *Ws* represents the swollen hydrogel disc's weight at a certain period.

Rheological analysis

Steady rheological behaviour

The rheological characteristics of CMGT-co-SAH and SAH were assessed in the swollen state in PBS buffer of pH 7.4 at room temperature using an Anton Paar Modular Compact Rheometer 302 (MCR). The shear rate ranged from 0.001 to 1 s^{-1} with a PP-25 i.e., parallel plate having a diameter of 25 mm and along with 2.5 mm of the inter-platen gap. The results from the plot, shear vs. shear rate, were fitted to Power Law (PL) model to acquire the required parameters.

$$\text{PL model: } \tau = K\gamma^n \quad \ldots (4)$$

The shear stress (τ) in (Pa), consistency coefficient (K) in (Pa.s), shear rate (γ) in (s^{-1}), and fluidity index (n) are all represented in the equation (4)[21].

Amplitude sweep

The test for amplitude sweep was done on SAH and CMGT-co-SAH in an oscillatory condition at a frequency of 10 $rads^{-1}$ to optimize suitable parameters for further dynamic testing. The amplitude sweep test is conducted in a fixed strain % of 0.001 % to 10 %. The test may reveal the linear viscoelastic region (LVR), which may be used to examine sample characteristics.

Frequency sweep

Low and high frequencies (1-100 rad s^{-1}) and (100-1000 rad s^{-1}) respectively, were used in the frequency sweep test. For CMGT-co-SAH and SAH, the loss (G″) and storage (G′) moduli are plotted against (ω) angular frequency at room temperature.

SEM

Morphology of four samples (GT, CMGT, SAH and CMGT-co-SAH) was compared by using JEOL JSM-6610LV Scanning Electron Microscope and all samples were coated with gold for analysis. SEM was operated at 20 kV accelerating voltage and 1,000x magnifications[22].

FTIR

FTIR of CMGT-co-SAH were compared with GT, CMGT and SAH. The FTIR analysis of samples was done between range 4000 to 650 cm^{-1} on Perkin-Elmer model 2000 FT-IR spectrometer[23].

^{13}C NMR

Solid state^{13}C-NMR was done for four samples, i.e., GT, CMGT, SAH and CMGT-co-SAH with 200 mg of samples at 9T of magnetic field on a Bruker Avance 500 WB solid state NMR spectrometer using 4mm of the probe[24].

XRD

The samples (GT, CMGT, SAH and CMGT-co-SAH) X-Ray Diffract gram we rerecorded by diffracting angle from 10° to 80° at 2°/min with 40 KV generator voltage using Expert Pro MRD, Panalytical, X-Ray diffractometer[25].

TGA

The samples (GT, CMGT, SAH and CMGT-co-SAH) were thermally tested with a consistent heating rate of 10°C/min from 25 to 800°C in N_2 atmosphere, using a PerkinElmer TGA, 4000[26].

Analysis of network parameters of CMGT-co-SAH

The AFS amount released from the hydrogel matrix is determined by the hydrogel's swelling,

which is directly related to the network parameters like Molecular weight of the segments between two neighbouring crosslinks of the network hydrogel ($\overline{Mc}$), the volume fraction of the swollen hydrogel (ϕ), mesh size (ξ), Flory Huggins interaction parameter (χ) and crosslink density (ρ). These parameters were calculated by Flory-Rehner equation given in equation 5[27].

$$\overline{Mc} = -D_H + \mathrm{V}m + \phi^{\frac{1}{3}} [\ln(1-\phi) + \phi + \chi\phi^2]^{-1} \quad \ldots (5)$$

Here, ϕ represents the swollen hydrogel's volume fraction, Vm represents the molar volume of the swelling agent, which determine the amount of solvent absorbed by the hydrogel and the Flory Huggins interaction parameter is represented by χ. ϕ, for swollen hydrogel, was calculated using equation (6).

$$\phi = \left[\left(\frac{D_H}{D_S}\right)\left(\frac{\mathrm{Ws}-\mathrm{Wi}}{\mathrm{Wi}}\right) + 1\right]^{-1} \quad \ldots (6)$$

Here, D_S and D_H are the densities of the solvent (g/cm^3) and hydrogel, respectively. Wi and Ws are the weight of initial and swollen state of the hydrogel.

The Flory Huggins interaction parameter (χ) was determined by using the equation (7)

$$\chi = \left(\phi\left({}^{1}/_{1-\phi}\right) + \mathrm{Z}\ln(1-\phi) + \mathrm{Z}\phi\right)[2\phi - \phi 2\mathrm{Z} - \phi 2\mathrm{T} - 1 d\phi/dT - 1 - 1 \quad \ldots (7)$$

where

$\mathrm{Z} = \left[\left(\frac{\phi^{\frac{2}{3}}}{3} - \frac{2}{3}\right)\left(\phi^{\frac{1}{3}} - \frac{2\phi}{3}\right)\right]^{-1}$ and $d\phi/dT$ is the slope calculated by plotting a graph between temperature in °C and volume fraction ( ). 24 h swelling of hydrogel was determined at 27°, 37° and 47°C in buffer of pH 7.4. Mesh size and Crosslink density were determined by using the given equation (8,9)[28,29].

$$\rho = \frac{D_H}{\overline{Mc}} \quad \ldots (8)$$

$$\xi = \left[\left(\frac{71}{1000}\right)(\phi)^{-\frac{1}{3}}\right](\overline{Mc})^{\frac{1}{2}} \quad \ldots (9)$$

Drug loading and release profile

The AFS loading and release profile of CMGT-co-SAH was determined in *p*H 7.4 buffer solution at 37°C. The swelling equilibrium approach was used to load the drug into the hydrogel[30]. For 24 hours, the hydrogel was immersed in a drug solution with a fixed concentration (1.25 mg/mL). The drug-loaded hydrogel was immersed in a buffer solution of *p*H 7.4 in a beaker and placed in a water bath shaker, set at 80 rpm and 37°C, to analyze the release profile of hydrogel. After an interval of time, 1ml of the drug containing solution was taken out and replaced by a fresh buffer solution. The process was continued for 24 h. The withdrawn samples were analyzed by a UV -visible spectrometer at 274 nm. The amount of AFS was measured by comparing the absorbance value from the calibration curve. The experiment was conducted in triplicates and drug release kinetics was analyzed by applying various drug release models. The Encapsulation Efficiency (EE)was observed using the formula, given in equation 10[31].

$$\%\ \text{of EE} = \left(\frac{\text{Actual loading}}{\text{Theoretical loading}}\right) \times 100 \quad \ldots (10)$$

Kinetic models for Drug release profile

To determine the drug release profile of AFS loaded CMGT-co-SAH, Higuchi, Hixon-Crowell, Korsmeyer-Peppas, First-order and Zero-order kinetic models were employed[20,32]. Mathematical equations of the models have been given in Table 2.

Hemo-compatibility studies

The hemolytic potential of hydrogel was determined by an *in vitro* hemolytic index. The blood sample was collected from healthy human in EDTA

Table 2 — Mathematical expression of kinetic models.

Models	Mathematical equation	Parameter
Zero Order	$F_t = K_o t$	F_t=Amount of drug release in time *t* K_o= Zero-order constant
First Order	$(1 - F_t) = K_1 t$	K_1= First order constant
Higuchi	$F_t = K_H t^{1/2}$	K_H= Higuchi constant
Hixon-Crowell	$W_o{}^{1/3}$-$W_t{}^{1/3} = K_{HC} t$	W_o=Initial amount of drug present in hydrogel W_t=Amount of drug release at time t K_{HC}= Hixon-crowell constant
Korsmeyer-Peppas	$\frac{M_t}{M_\infty} = K_{KP} t^n$	$\frac{M_t}{M_\infty}$=Amount of drug release in time *t* K_{KP}=Rate constant n= Release exponent

treated tubes and centrifuged for 5 min, at 3000 rpm. Supernatant of blood plasma was discarded, and separated RBCs were, washed in 1× PBS (*p*H 7.4), further resuspended in 1×PBS. For use in experiments this stock solution was diluted to 4% v/v in 1×PBS.Triton X-100 was used as the positive control (0.1%w/v) and 1×PBS (pH 7.4) act as negative control[33].

The hemolysis in % was calculated by using equation 11:

$$\text{Hemolysis in \%} = \left(\frac{A_{CMGT-co-SAH} - A_{1xPBS}}{A_{triton\ X-100} - A_{1xPBS}}\right) \times 100 \quad \ldots (11)$$

Hemolysis in % was evaluated on average of two replicates[34].

Results and Discussion

Swelling studies

CMGT-co-SAH formulations 1-11 were synthesized by varying concentrations of KPS and MBA where monomer and polysaccharides concentrations were not changed. Their swelling index was determined. The formulation which is having maximum SI has been used to determine the effect of change in temperature on swelling of the hydrogel.

Effect of cross-linker on hydrogel's swelling

The effect of cross-linker's concentration was observed in samples (CMGT-co-SAH-1 to 6 listed in Table 1, shown in Fig. 1(a). Swelling Index increases when the cross-linker concentration increases from 0.01mol/L to 0.017 mol/L due to a rise in cross-linked density beyond which the swelling index decreases. This may be due to the occurrence of rigid structure, beyond cross-linker concentration of 0.017 mL/L which causes a reduction in polymer stretching.

Effect of initiator on hydrogel's swelling

According to Fig. 1(b), as the initiator concentration increases, the anionic radical increases. Anionic radical will increase macro-radicals in the parent chain, which raises the swelling Index to

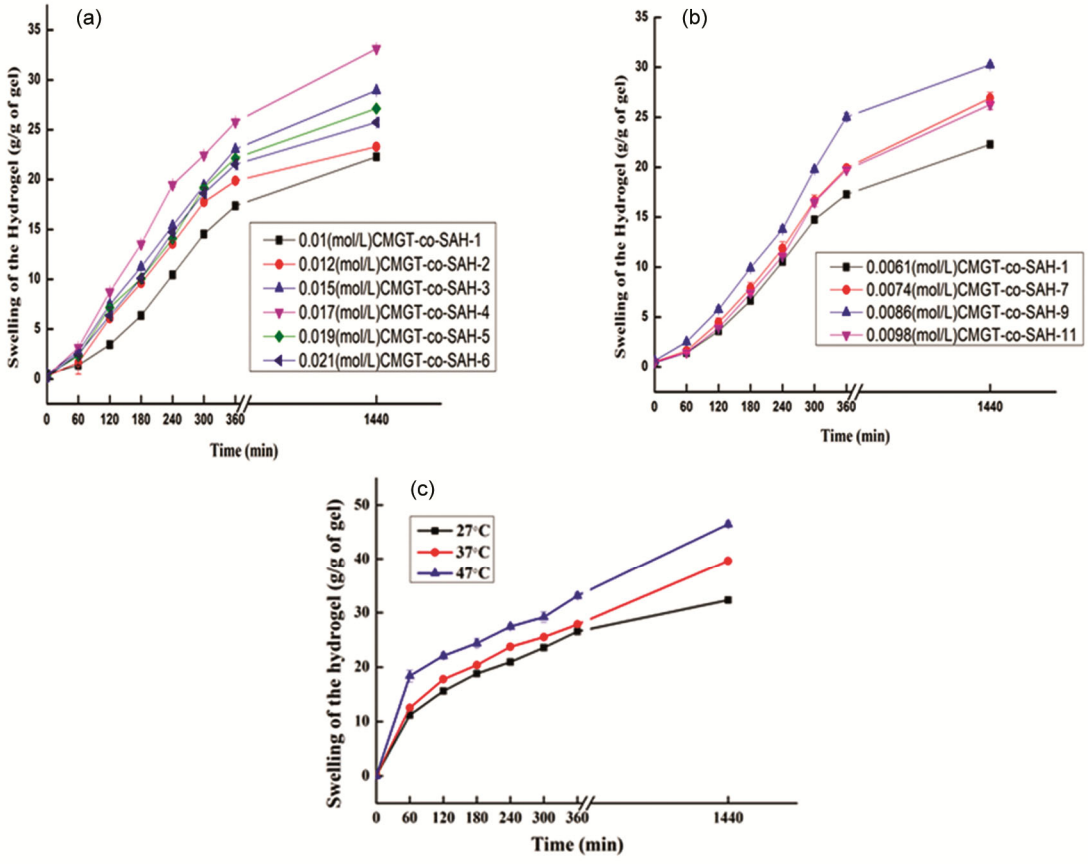

Fig. 1 — (a) Effect of cross-linker on hydrogel's swelling; (b) Effect of initiator on hydrogel's swelling and (c) Effect of temperature on hydrogel's swelling.

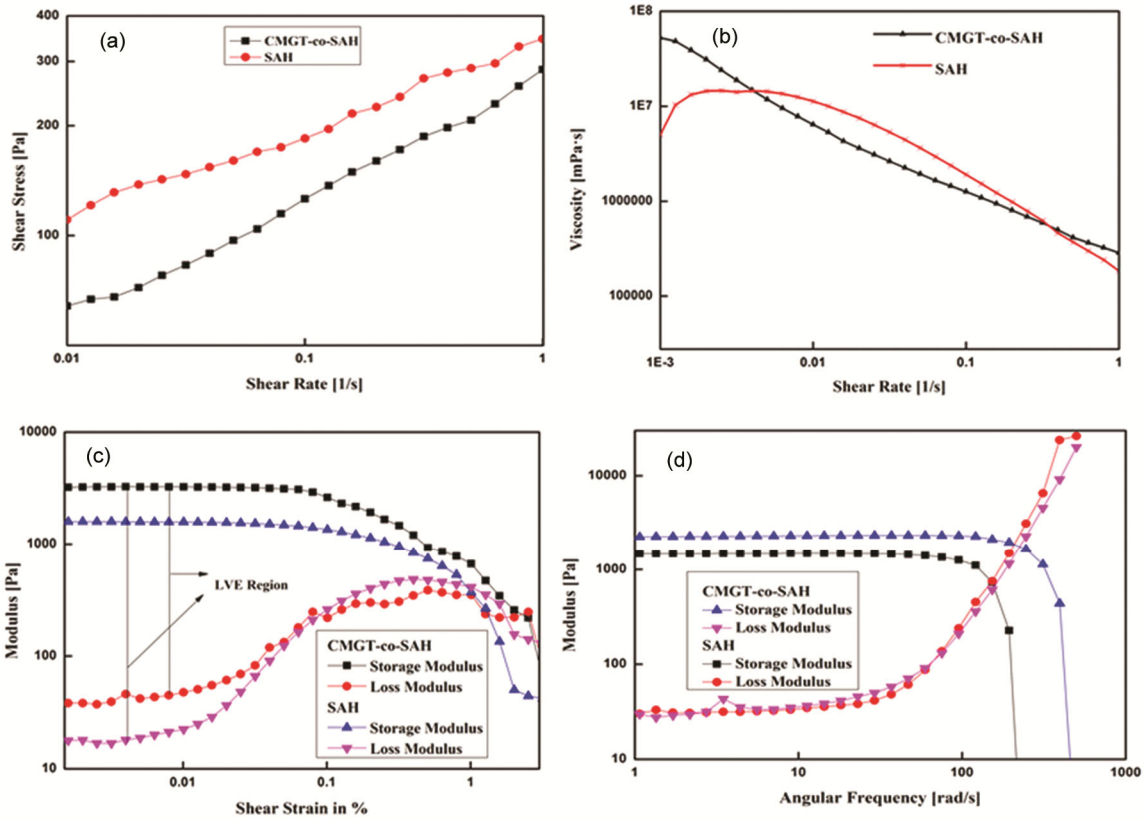

Fig. 2 — (a) Shear rate versus Shear stress graph for CMGT-co-SAH and SAH; (b) Viscosity profile of CMGT-co-SAH and SAH with varying shear rate; (c) Amplitude sweep with LVE and (d) frequency sweep graphs.

30.25±0.19 g/g (CMGT-co-SAH-1, 7, 9 and 11) listed in table 1 (where cross-linker concentration is constant). Further, with increase in the concentration of initiator beyond 0.0086 mol/L, swelling index decreases due to termination of the chain through the biomolecular collision.

Effect of temperature on hydrogel's swelling

The SI (g/g of gel) at 27°, 37° and 47° was found to be 32.30±0.12, 39.63±0.30, 46.47±0.54 respectively. It was observed from results that as the temperature increases, hydrogel's swelling increases (Fig.1(c)) due to increase in movement of the segments of the polymerized chains. This confirms that the rate of absorption/diffusion of solvent molecules by CMGT-co-SAH is temperature dependant.

Rheological analysis

The gel strength and rigidity of the swollen hydrogel were determined by using rheological analysis. From Fig. 2(a), in which the graph was plotted against shear stress and shear rate, for both hydrogels (CMGT-co-SAH and SAH), it was observed that the shear stress is directly proportional to shear rate. For data (shear rate vs. shear stress graph), the PL model was fitted to calculate the consistency coefficient (K) and fluidity index(N).The value of R^2 obtained from the PL model indicates that both the hydrogels have high consistency and correlated with reported results in the previous literature[35]. The value of 'n' shows flow characteristics, when obtained results of shear rate versus shear stress was fitted to the PL model. The value of 'n' in Table 3 is more for CMGT-co-SAH than SAH, representing the intermolecular interaction of the monomer and the CMGT. The value of n for both hydrogel is less than one, which means pseudo-plastic behaviour of the hydrogel. This behaviour was also determined by the shear viscosity test, Fig. 2(b). The hydrogel showed a steady decrease in shear-dependent viscosity with an increase in shear rate,

Table 3 — Parameters according to Power law model in steady rheological behaviour (shear stress vs. shear rate).

	Power law model		
Hydrogel	K	N	R^2
SAH	11.70	0.23	0.9907
CMGT-co-SAH	11.35	0.33	0.9946

which might indicate the time-dependent rupturing of the hydrogel matrix's intrinsic bonding, thus representing the shear thinning behaviour of hydrogel.

Amplitude sweep

The whole strain was divided into two regions. One is the Linear Viscoelastic Region (LVR), a shear region, which is not affected by applied stress. The other area is non-linear and it was observed from Fig. 2(c) that the G' and G" values change when the strain exceeds 0.01%. Above this LVR, the storage and the loss modulus dropped due to rupturing of the hydro gel matrix. By increasing the stress %, intermolecular interaction deformed, reducing the moduli values. Samples act as viscoelastic solid when G'>G". Below 0.01% strain, the shape of CMGT-co-SAH&SAH was retained. Above 0.01% strain, intermolecular chains start to disentangle. The yield strain of CMGT-co-SAH is more than SAH due to the addition of CMGT, which shows intermolecular interaction of CMGT and SA. Similar properties were observed by Ganguly et al. in psyllium grafted with poly acrylic acid and sodium acrylate hydrogel[16]. The viscoelastic sweep should be analyzed within the LVE range[35].

Frequency sweep

For this analysis, the frequency ranged from 1 to 1000 rads^{-1}. Storage and loss moduli were plotted against (ω) i.e., angular frequency Fig. 2(d). The graph shows viscoelastic solid behaviour, where the loss modulus is dominant at high frequencies and the storage modulus is prominent at low frequencies. Therefore the structure of the hydrogel is stable at low frequency and deformed at high frequency. CMGT-co-SAH has a greater storage modulus than SAH because there may be crosslinking between SA and CMGT. It shifts the cross-over point toward a higher frequency[16,36].

Scanning Electron Micrograph (SEM)

The surface morphology of GT, CMGT, SAH and CMGT-co-SAH has been analyzed by SEMs, which are represented in Fig. 3. It has been observed from the SEMs that GTand SAH have a smooth and homogeneous morphology, whereas CMGT and CMGT-co-SAH have structural heterogeneity and porous morphology. The change in surface morphology of the CMGT and its hydrogel is due to the cross-linked networks confirmed by SEMs taken at 1000x magnification[6,37].

FTIR Analysis

Peaks observed from FTIR spectra were compared with previously published literature as given in Fig. 4 (a). A broad absorption band at 3311 cm^{-1} was observed in GT, representing an overlapped peak indicating H-bond due to -OH groups of polysaccharides. Absorption bands at 1720 cm^{-1} in GT represent a stretch of acidic and ester carbonyl groups and at 1602 cm^{-1} represent C-O and COO^{-} groups of D-Glacturonic acid. The peak at 1247 cm^{-1} represents the esteric skeleton group. Stretch at 1029cm^{-1} corresponds to C-O and C-C group present in GT's pyranose rings[12].

The broad absorption band at 3329 cm^{-1} in CMGT and GT, but band intensity is lower in CMGT than GT, suggests that carboxymethylation may reduce the number of –OH groups. A band at 1600 cm^{-1}representsthe extension vibration of the COO^{-} groups, which confirms the carboxymethylation process. Other absorption bands at 1244 cm^{-1} and

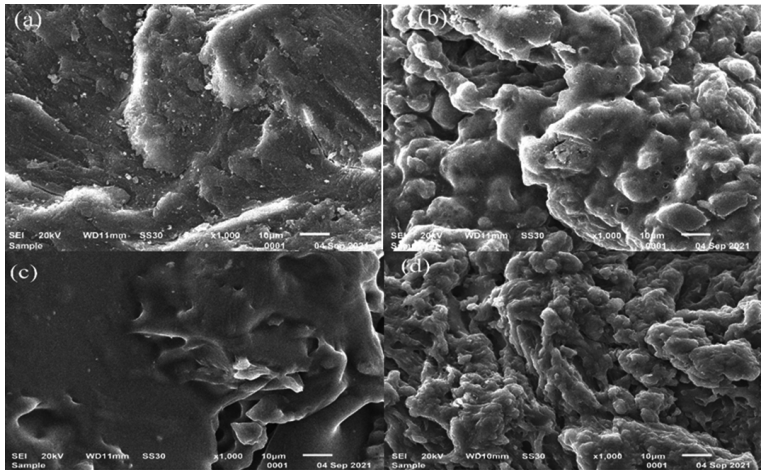

Fig. 3 — SEM at (1000x) for (a) GT; (b) CMGT; (c) SAH and (d) CMGT-co-SAH.

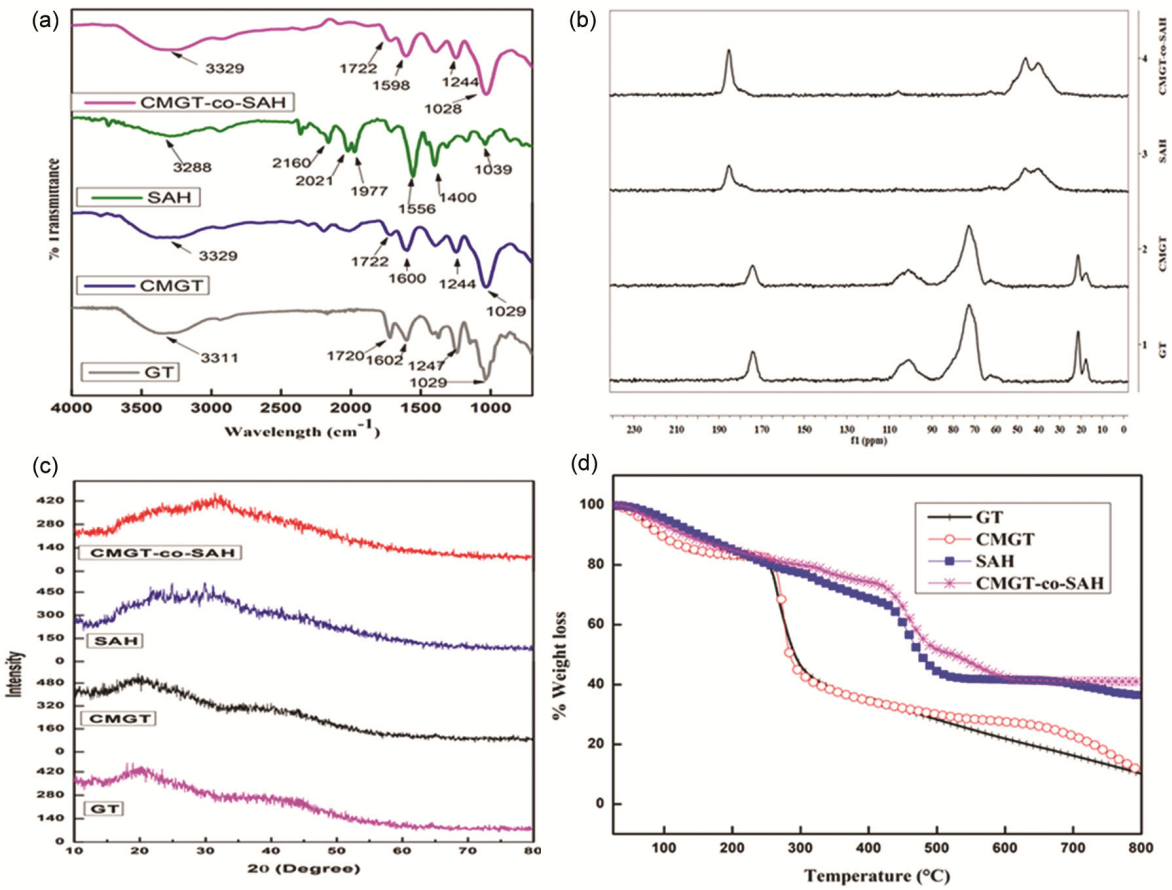

Fig. 4 — (a) FTIR; (b) ^{13}C-NMR; (c)XRD and (d) TGA spectra of GT, CMGT, SAH and CMGT-co-SAH.

1029 cm^{-1} are corresponding to the similar vibrations of GT as explained above[38].

SAH's FTIR spectrum represents absorption bands at 1556 cm^{-1}and 1400 cm^{-1}due to the bending vibrations of the CH_2 group of sodium acrylate parts[39].

In the CMGT-co-SAH's spectrum, the absorption band at 3329 cm^{-1} corresponds to the acidic -OH group overlapped with the amide -NH group. Absorption bands at 1722 cm^{-1} represent the stretch of acidic and ester carbonyl groups and at 1606 cm^{-1} are due to the amide carbonyl group. Absorptions at 1244 cm^{-1} and 1028 cm^{-1} are assigned as of CMGT. A little shift in absorptions confirms the crosslinking of CMGT with sodium acrylate[37].

^{13}C-NMR studies

The result of solid-state ^{13}C-NMR spectra of GT, CMGT, SAH and CMGT-co-SAH are shown in Fig. 4(b). At 174.24 ppm, characteristic peaks have been identified in GT due to the -COOH group of galacturonic acid in the GT[32].At 100.59 ppm (represents anomeric carbon of polysaccharides), at 72.56 ppm (due to C attached to-OH group of polymeric chain), 17-22 ppm (assigned to -CH_3 and -CH_2 group of polysaccharides). NMR spectrum of CMGT represents characteristic peaks at 174.26 ppm (carbonyl carbon of CMGT), at 101.04 ppm (anomeric carbon of polysaccharides). This peak shifted to a higher ppm value than GT may be due to carboxymethylation. Peak at 72.71 ppm due to –C-OH group, peak intensity lower down as compared to GT, confirms carboxymethylation. In SAH, characteristic peaks from 40-47 ppm and 185.51 ppm assigned to -CH and -COOH group, respectively. In CMGT-co-SAH, characteristics peaks from 40-47 ppm assigned to -CH of sodium acrylate and little shift in frequency confirmed crosslinking of CMGT with SA. At 106.05 ppm small intensity peak was identified, representing anomeric carbon of polysaccharides. At 185.38 ppm (-COOH of SA and CMGT, a shift in frequency due to crosslinking of CMGT with SA)[6,32].

XRD studies

Figure 4(c) represents the crystallinity/amorphous characteristics of the samples, analyzed by XRD. The GT showed a broad diffraction peak at ≈20°, indicating that it is an amorphous polysaccharide, and there is little shift in the 2θ value due to carboxymethylation. The diffraction pattern of SAH and CMGT-co-SAH show the amorphous nature. The shift in the diffraction peak of CMGT-co-SAH was observed, may be due to cross-linking of CMGT and SA[40,41].

TGA

Figure 4(d) represents the thermal degradation of GT, CMGT, SAH and CMGT-co-SAH. GT demonstrates two-step weight loss, with an initial loss of around 18% between 39 - 234°C due to the loss of moisture from the gum. The decomposition of GT's highly branched heterogeneous structure results in a 72 % weight loss from temperature 234°C to 800°C, with a residual weight of about 10%.

CMGT decomposes in three stages, 35-240°C,the range shows 16% loss due to humidity. The second stage ranges from 240-620°C due to decomposition of polysaccharide rings, breaking of C-O-C bond in CMGT chain and elimination of CO_2, which is around 74%. 620-800°C range shows weight losses due to breakdown of CMGT backbone and 10% were residual weight.

Thermal decomposition of SAH occurs in four stages, 30-299°C, 299-427°C, 427-548°C, 672-800°C and were about 23%, 11%, 25% and 5% respectively. The first stage weight loss was result of loss of moisture. The second stage of weight loss was due to carboxyl group decomposition of the SAH and the last two stages show the breakage of cross-linking in SAH network. 36% is the residual weight at 800°C.

CMGT-co-SAH decomposed in four stages 44-322°C, 322-411°C, 411-521°C, and 521-629°C. The first stage shows 21% loss due to moisture content. The second stage of 6% loss represents the decomposition of polysaccharide rings along with the elimination of CO_2. The latter two stages represent breakage of the CMGT backbone and SA chain with 23% and 9% weight loss respectively. The residual weight at 800°C was 41%. From the decomposition of all samples, it was concluded that modified gum and its hydrogel were more thermally stable than GT and SAH[17,42].

Network parameters of hydrogel

The network parameters like (Molecular weight of the segments between two neighbouring crosslinks ($\bar{M}_c$), the volume fraction of the hydrogel in the swollen state (ϕ), mesh size (ξ), Flory Huggins interaction parameter (χ) and crosslink density (ρ)) of CMGT-co-SAH were determined as a function of temperature and given in Table 4. When a hydrogel is immersed in a liquid for swelling, it expands until the osmotic forces that aid in the polymer's dissolution is counterbalanced by the elastic forces caused by stretched polymer chains. High $\bar{M}_c$ value shows that the network is highly elastic and expands quickly when exposed to a liquid solvent[27]. As the temperature increases, $\bar{M}_c$ and ξ of the hydrogel network increases along with that ρ and χ decreases[43].

AFS release studies

The encapsulation efficiency of the loaded hydrogel found out to be 63.8% and the release studies of AFS from AFS-loaded-CMGT-co-SAH were determined in a buffer solution of *p*H 7.4, AFS is soluble in buffer of *p*H 7.4 therefore 7.4 *p*H buffer was selected for release study. Also, the swelling of the hydrogel is maximum in *p*H 7.4 buffer. Here, the two factors, the solubility of the drug and swelling of the hydrogel are responsible for the diffusion of the drug. Generally, the release/swelling of drug/ hydrogelis co-related with the cross-linked matrix of monomer and polysaccharides, nature of the solvent, density and composition of the hydrogel[28]. The rate was reasonably rapid during the early phases of drug release from the hydrogel, as shown in Fig. 5(a). After that, it demonstrated controlled and sustained release. The rate of drug release decreases with an instant of time. It was observed from the release data that 52.2% of the loaded drug was released from the matrix in early time interval. It might be because the drug on the surface of the polymer matrix releases faster than the drug integrated into the polymeric matrix, allowing for controlled drug delivery from the hydrogel. The results reveals that the release of the drug from the hydrogel is related to the swelling of the hydrogel and follows the Fickian mechanism[44]. The kinetics were further investigated by fitting the obtained drug release data to several mathematical models. Fig. 5(b) and Table 5, shows that the highest correlation coefficient(R^2)value was found in the Korsmeyer-Peppas model, representing drug release from a polymeric system. The measured 'n' value is 0.4176 given in table 5, less than 0.5 and corresponds to the Fickian mechanism of drug release[45], in which the driving force is a chemical gradient and the release

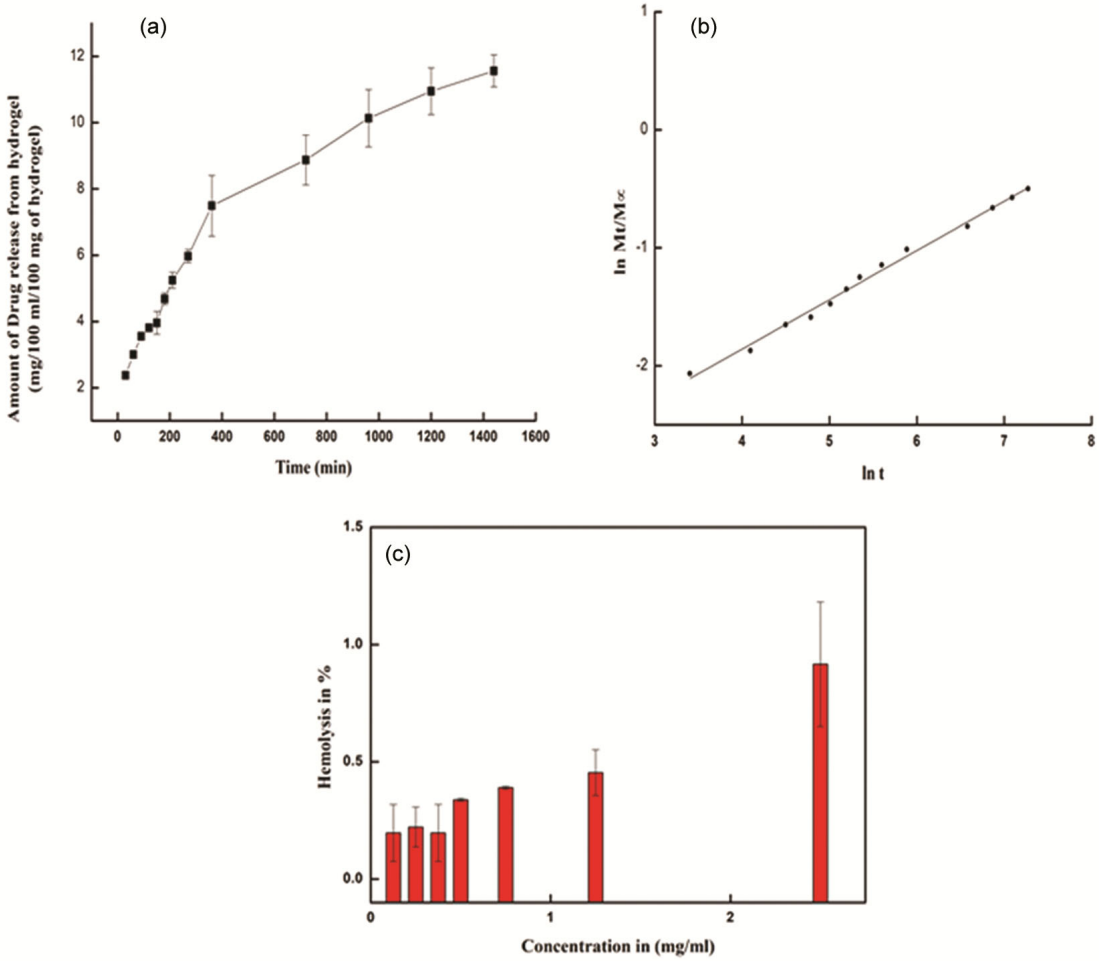

Fig. 5 — (a) Release profile of AFS from CMGT-co-SAH; (b) Graph between $ln\frac{M_t}{M_\infty}$ and *ln*t for determination of the rate constant and rate exponent and (c) Hemo-compatability studies.

Table 4—Network parameters of CMGT-co-SAH as a function of temperature.

Temperature (°C)	Φ	X	$\bar{M}_c$(g/mol)	ρ (mol/cm^3)	ξ (nm)
27	0.042079	0.217329772	8458	8.3578	18.773
37	0.034604	0.239979899	12807	5.5194	24.657
47	0.028767	0.261771407	19100	3.7010	32.024

Table 5 — Different models to study drug release kinetics of AFS from CMGT-co-SAH

Models	R^2	K	N
Zero-order	0.9344	K_o (min^{-1}) 0.03251±0.0024	
First-order	0.9292	K_1 (min^{-1}) 0.11515±0.0040	
Hixon-Crowell	0.9344	K_{HC}($min^{-1/2}$) 0.002±1.55	
Higuchi	0.9919	K_H($min^{-1/3}$) 1.48271±0.038	
Korsmeyer-Peppas	0.9933	K_{KP}(min^{-n}) 0.029348±0.005	0.4176

mechanism is diffusion-controlled[31]. The Higuchi model also supports the fickian diffusion of the drug from the hydrogel polymeric matrix.

Hemo-compatibility studies

Hemolytic potential of CMGT-co-SAH was evaluated (Table 6) and results was plotted shown in Fig. 5(c). The evaluated results show that % hemolysis is less than 1 at every concentration. In general, the sample shows %hemolysis less 5 is highly hemo-compatible and may be good for pharmaceutical application[46].

Table 6 — Hemocompatibility studies result.

CMGT-co-SAH Concentration(mg/mL)	Haemolysis in %	Remarks
0.125	0.1965±0.12	Highly hemocompatible
0.25	0.2223±0.08	Highly hemocompatible
0.375	0.1965±0.12	Highly hemocompatible
0.5	0.3381±0.006	Highly hemocompatible
0.75	0.3895±0.006	Highly hemocompatible
1.25	0.4539±0.09	Highly hemocompatible
2.5	0.9164±0.26	Highly hemocompatible

The results obtained from Hemolysis test show that CMGT-co-SAH is highly hemocompatible shown in Fig. 5(c) and Table 6 and all the reactants used to synthesize CMGT-co-SAH previously been reported as safe and non-toxic to the environment. Recently, cytocompatibilities of GT and Acrylic acid based hydrogel by MTT assay was confirmed by Sayadnia *et al.*[41]. Khan and Anwar have proven that carboxymethylation does not have any cytotoxic effects[47]. N,N′-methylenebis(acrylamide) used in the synthesis of CMGT-co-SAH is also safe for drug delivery[48].

Conclusion

The current investigation focused on the structural modification of natural gum into its carboxymethylated derivative and the subsequent fabrication of CMGT-co-SA Hydrogel by graft copolymerization technique. The synthesized CMGT-co-SAH shows more stability than SAH, revealed by characterization performed by using an optimum formulation (CMGT-co-SAH-4).The investigation reveals that cross-linker and initiator concentration affect the swelling of the hydrogel. Molecular weight and mesh size between two neighbouring crosslinks increase with the increase in temperature. The elasticity of SAH was less than CMGT-co-SAH as (G'/G") was raised with the addition of CMGT to the hydrogel. The hemolysis test result confirms the hemocompatible nature of the hydrogel. The drug release from the hydrogel loaded with the non-steroidal anti-inflammatory drug, aceclofenac sodium follows the Fickian diffusion mechanism. It is best fitted in Korsmeyer-Peppas and Higuchi models. Thus it can be concluded that synthesized hydrogel is suitable for the controlled release of drug molecules.

Acknowledgements

The authors would like to acknowledge Dr. Santosh Yadav (Institute of Genomics and Integrative Biology, Mall road, New Delhi-110007) for carrying out Hemolysis test for the synthesized CMGT-co-SAH, Tata Institute of Fundamental Re-search Hyderabad, Gopanpally, Hyderabad-500107, Telangana, India for ^{13}C-NMR spectroscopy. The authors are also thankful to Vice Chancellor, DTU for providing financial assistance and research facility and to Dr. Manish Jain (Delhi Technological University) for helpful discussion.

References

1 Bajpai A & Raj V, *Polym Bull*, 78 (2021) 4109.
2 Sharma B, Bharti R & Sharma R, *Mater Today Proc*, 65 (2022) 3657.
3 Singh B, Sharma V, Kumar R & Mohan M, *Food Hydrocoll Heal*, 2 (2022) 100059.
4 Nejatian M, Abbasi S & Azarikia F, *Int J Biol Macromol*, 160 (2020) 846.
5 Nazarzadeh Zare E, Makvandi P & Tay F R, *Carbohydr Polym*, 212 (2019) 450.
6 Singh B & Sharma V, *Carbohydr Polym*, 157 (2017) 185.
7 Tischer C A, Iacomini M & Gorin P A J, *Carbohydr Res*, 337 (2002) 1647.
8 Polez R T, Morits M, Jonkergouw C, Phiri J, Valle-Delgado J J, Linder M B, Maloney T, Rojas O J & Österberg M, *Int J Biol Macromol*, 215 (2022) 691.
9 Verma C, Negi P, Pathania D, Sethi V & B Gupta, *Polym Int*, 68 (2019) 344.
10 Rimpy, Abhishek & Ahuja M, *Carbohydr Polym*, 174 (2017) 896.
11 Sullad A G, Manjeshwar L S & Aminabhavi T M, *J Appl Polym Sci*, 122 (2011) 452.
12 Veeramachineni A K, Sathasivam T, Paramasivam R, Muniyandy S & Pushpamalar J, *J Polym Environ*, 27 (2019) 1516.
13 Wang Q, Qu Y, Zhang Z, Huang H, Xu Y, Shen F, Wang L & Sun L, *Gels*, 8 (2022) 400.
14 Chang C & Zhang L, *Carbohydr Polym*, 84 (2011) 40.
15 Jabbari E & S Nozari, *Eur Polym J*, 36 (2000) 2685.
16 Ganguly S, Mondal S, Das P, Bhawal P, Maity P P, Ghosh S, Dhara S & Das N C, *Int J Biol Macromol*, 111 (2018) 983.
17 Behrouzi M & Moghadam P N, *Carbohydr Polym*, 202 (2018) 227.
18 Santos M B, dos Santos C H C, de Carvalho M G, de Carvalho C W P & Garcia-Rojas E E, *Int J Biol Macromol*, 134 (2019) 595.
19 Verma S & Ahuja M, *Int J Biol Macromol*, 98 (2017) 75.
20 Suhail M, Wu P C & Minhas M U, *J Saudi Chem Soc*, 25 (2021) 101212.
21 Fan Z, Cheng P, Zhang P, Gao Y, Zhao Y, Liu M, Gu J, Wang Z & Han J, *Int J Biol Macromol*, 208 (2022) 1.
22 Tanpichai S, Phoothong F & A Boonmahitthisud, *Sci Rep*, 12 (2022) 1.
23 Kannaujia R, Prasad V, Sapna, Rawat P, Rawat V, Thakur A, Majumdar S, Verma M, Rao G K, Gupta A P, Kumar H & Srivastava C M, *Mater Lett*, 252 (2019) 198.
24 Singh B, Sharma V & Kumar A, *Carbohydr Polym Technol Appl*, 2 (2021) 100062.
25 Malik S & Ahuja M, *Carbohydr Polym*, 86 (2011) 177.
26 Badwaik H R, Sakure K, Alexander A, Ajazuddin, Dhongade H & Tripathi D K, *Int J Biol Macromol*, 85 (2016) 361.

27 Kulkarni A R, Soppimath K S, Aminabhavi T M, Dave A M & Mehta M H, *J Control Release*, 63 **(**2000**)** 97.
28 Singh B & Singh B, *Int J Biol Macromol*, 99 **(**2017**)** 699.
29 Chung J T, Vlugt-Wensink K D F, Hennink W E & Zhang Z, *Int J Pharm*, 288 **(**2005**)** 51.
30 Singh B & Singh B, *Int J Biol Macromol*, 99 **(**2017**)** 699.
31 Goel H, Gupta N, Santhiya D, Dey N, Bohidar H B & Bhattacharya A, *Int J Biol Macromol*, 174 **(**2021**)** 240.
32 Singh B & Sharma V, *Polymer (Guildf)*, 91 **(**2016**)** 50.
33 Suryadevara V, Lankapalli S R, Thalamanchi B, Patcha A & Danda L H, *Asian J Pharm*, 10 **(**2016**)** 51.
34 Pal K & Pal S, *Mater Manuf Process*, 21 **(**2006**)** 325.
35 Fan Z, Cheng P, Gao Y, Wang D, Jia G, Zhang P, Prakash S, Wang Z & J Han, *Food Hydrocoll*, 123 **(**2022**)** 107162.
36 Yadav R & Purwar R, *Polym Test*, 93 **(**2021**)** 106916.
37 Bachra Y, Grouli A, Damiri F, Talbi M & Berrada M, *Int J Biomater*, 2021 **(**2021**)** 1.
38 Hasan A M A, Keshawy M & Abdel-Raouf M E S, *Mater Chem Phys*, 278 **(**2022**)** 125521.
39 Santos F B, Miranda N T, Schiavon M I R B, Fregolente L V & Wolf Maciel M R, *J Therm Anal Calorim*, 146 **(**2021**)** 2503.
40 Singh B, Varshney L, Francis S & Rajneesh, *Int J Biol Macromol*, 88 **(**2016**)** 586.
41 Sayadnia S, Arkan E, Jahanban-Esfahlan R, Sayadnia S & Jaymand M, *Polym Adv Technol*, 32 **(**2021**)** 262.
42 Wang W & Wang A, *J Appl Polym Sci*, 112 **(**2009**)** 2102.
43 Singh B & Singh B, *Int J Biol Macromol*, 159 **(**2020**)** 264.
44 Singh B & Rajneesh, *J Drug Deliv Sci Technol*, 47 **(**2018**)** 200.
45 Mukherjee K, Dutta P & T K Giri, *Int J Biol Macromol*, 232 **(**2023**)** 123448.
46 American Society for Testing and Materials, ASTM F 756-00, *Am Soc Test Mater*, **(**2000**)** 159.
47 Khan S & N Anwar, *Carbohydr Polym*, 257 **(**2021**)** 117617.
48 Lakouraj M M, Rezaei M & Hasantabar V, *Int J Biol Macromol*, 193 **(**2021**)** 609.